NJC

Accepted Manuscript

This is an *Accepted Manuscript*, which has been through the Royal Society of Chemistry peer review process and has been accepted for publication.

Accepted Manuscripts are published online shortly after acceptance, before technical editing, formatting and proof reading. Using this free service, authors can make their results available to the community, in citable form, before we publish the edited article. We will replace this *Accepted Manuscript* with the edited and formatted *Advance Article* as soon as it is available.

You can find more information about *Accepted Manuscripts* in the Information for Authors.

Please note that technical editing may introduce minor changes to the text and/or graphics, which may alter content. The journal's standard Terms & Conditions and the Ethical guidelines still apply. In no event shall the Royal Society of Chemistry be held responsible for any errors or omissions in this *Accepted Manuscript* or any consequences arising from the use of any information it contains.

ROYAL SOCIETY OF CHEMISTRY

www.rsc.org/njc

Cite this: DOI: 10.1039/c0xx00000x

www.rsc.org/xxxxxx

ARTICLE TYPE

DFT and QTAIM study of the novel d-block metal complexes with tetraoxa[8]circulene-based ligand†

Nataliya N. Karaush,[a] Gleb V. Baryshnikov[a], Valentina A. Minaeva and Boris F. Minaev[a,b]

Received (in XXX, XXX) Xth XXXXXXXXX 20XX, Accepted Xth XXXXXXXXX 20XX

DOI: 10.1039/b000000x

A series of the transition metal (d-block metals) ions complexes with the tetraoxa[8]circulene-based ligand having one- and two-decker (sandwich-type) structure has been designed and studied in the framework of DFT approach. The quantum theory of atoms in molecules (QTAIM) was additionally applied for the studied complexes with the aim to evaluate their peculiar electronic features. The obtained results indicate that that the complexation process depends on matching of the transition metal cation size to the size of tetraoxa[8]circulene-formed cavity similarly to formation of the crown ether complexes. Coordination bonds of the d-block metal ions with the neighbouring oxygen atoms in the studied complexes can be interpreted as an intermediate type of interaction. The binding energy of the coordinative M–O bonds has been calculated both by the Espinosa equation and DFT additive scheme in order to confirm the high stability of the studied systems. If the size of metal cation is larger than the corresponding crown cavity the formation of two-decker complexes with the two tetraoxa[8]circulene-based ligands is possible. Such sandwich-type complexes possess the unusual cubic coordination polyhedron of the central metal ion bound with eight oxygen atoms. Moreover, these complexes are additionally stabilized due to the presence of π-stacking interactions between the two opposite tetraoxa[8]circulene parallel sheets. The synthesis of the proposed π-extended tetraoxa[8]circulene sheets and their metal-complexation ability attract a special attention because of their promising application as the potential biomimetic-type nanopores.

1. Introduction

The construction of new well-ordered and multifunctional systems by the molecular self-assembly strategy is an interesting field of the supramolecular chemistry[1] that provides a background for the design of future generation of nanoscale materials for the potential applications in biomedicine[2a,b], catalysis[2c], solar energy conversion[2d,e], optoelectronics[2f], energy-storage devices[2g] etc.[2h,i,j] The main advantage herein is a capability to control the self-organization process into the desired nanostructures by the usage of specially designed molecular building blocks. Therefore, a great interest in the synthesis of the diverse artificial nanosystems analogous to natural biomaterials occurs for the last years (see, for example, Ref. [3] in which the biomimetic graphene-based nanopores containing Oxygen atoms have been designed by Kang *et. al.*).

It is well known that self-assembly phenomenon provides the basis for a number of natural processes including protein folding, DNA transcribing formation of cell membranes, etc. An attractive feature of the self-assembled organic monolayers is their possible usage as a template matrix for the metal incorporation in order to create the novel metal-containing composite materials and complexes[4]. The metal atoms inserted into the such organic matrix can impart the unique properties (e.g., magnetic or electronic) to these materials.[5a,b]

Coordination of tailor-made macrocyclic ligands with relevant metal atoms opens up a wide range of complexes varieties.[5,6,7] (See for example Ref.[5e] in which Shiekh *et. al.*[5e] have discussed a novel thia-aza-oxo macrocycle Schiff base ligand (1,10-dithia-3,8,12,17-tetraoxo-4,7,13,16-tetraazacyclo-octadecane **a**, (Fig. 1) and its Cu(II), Co(II), Ni(II) and Mn(II) complexes (Fig. 1, **b**) by the [2+2] condensation of thiodiglycolic acid and ethylenediamine).

During the past decade the study of polyazamacrocyclic ligands and their metal complexes has been vigorously pursued.[6,7] By this way, Chan *et al.*[6] have reported a synthesis and structural characterization of the bis(benzimidazole) (BBZ) ligand (Fig. 1, ***c***) and a series of its transition-metal complexes (Fig. 1, ***d***). In the sequel, they have modified the structure of the parent BBZ macrocycle (Fig. 1, ***c***) and have obtained ligand **e** (Fig. 1) and its d-block metal complexes **f** (Fig. 1). The next examples of polyazamacrocyclic ligands are recently synthesized N-confused porphyrinoids[7a] which were synthesized by the introduction of the confused pyrrole rings into the normal and expanded porphyrins; one of them is presented in Fig.1, **g**.

Prompt development of the circulenes‡[8,9] and circulene-like compounds[10] has led to the design of the novel 2D circulene-based polymers. Recently, a series of new tetraoxa[8]circulene (TOC) based compounds has been designed in accordance with self-assembly principle[11a,b]. A little later, Sun *et al.*[11c] have

proved excellent stability, promising mechanical, electronic, optical and thermoelectric properties of these TOC-sheets. Another peculiarity of the TOC-sheets structure (Fig. 1, **h**) is the presence of crown ether cavity through which they can capture metal ions, which size correlates with the size of the macrocycle cavity, similarly to the crown ethers[12]. By the self-organization principle the N-analogues of TOC-sheet have been recently synthesized by Nakamura *et al.*[13] from the initial porphyrin building blocks. Such sheets are able to form multi-core Cu(II) complexes (Fig. 1, **i**) with a planar cyclooctatetraene core. Similar self-assembly phenomenon of the functional macrocyclic ligands has been experimentally observed for other transition metal complexes having one- and two-decker structure[14].

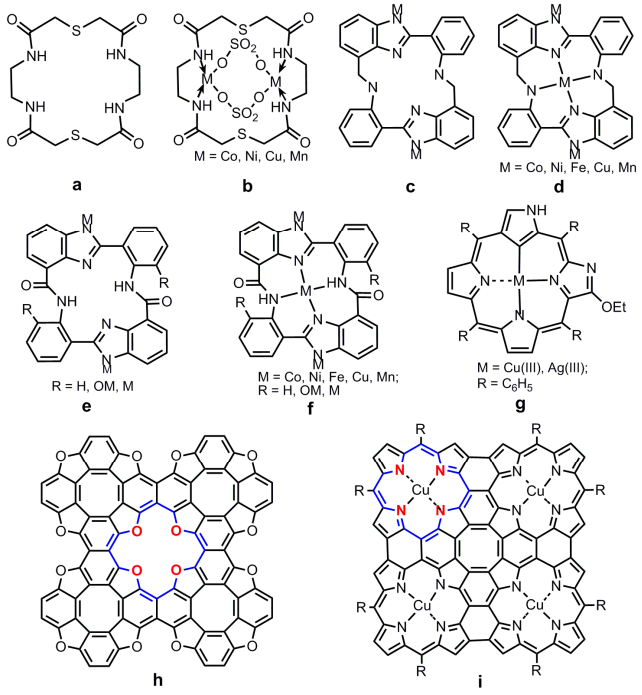

Fig. 1 Some examples of macrocyclic ligands and its complexes **a-g** and of the recently synthesized reactive building-blocks containing tetraoxa[8]circulene (**h**) and porphyrin (**i**) cores.

In the last few years the studies of some other metal complexes with the circulenes attract a considerable attention because of its fundamental and practical importance[15]. For example, [5]circulene (corannulene) represents the convex and concave face of bowl-shaped polyaromatic hydrocarbon (buckybowl) for the binding of metal centers and can be used as the multifunctional π-ligands from a coordination viewpoint[15]. Surprisingly, NMR investigations have shown that, in solution, a metal ion migrates around the curved surface of corannulene. For the first time it was observed by Angelici *et al.*[15g] in 2003. The same phenomenon was observed latter for other planar and nonplanar [n]circulenes.[15a-g]

In our recent paper we have described the selective s-block metal complexation with TOC-sheets.[16] This work continues and expands our previous investigation[16] in the context of exploring the complexation selectivity of d-block metal cations with the TOC-based ligand. It looks as a promising approach to the potential applications of TOC-sheets as synthetic ionic channels that makes actual their synthesis.

2. Method of calculation

The equilibrium geometry parameters of the studied complexes **1–6** (Fig. 2, 3) have been calculated by the DFT/B3LYP[17] method with the control of possible symmetry constrains using the effective core potential Lanl2DZ[18] basis set. Vibrational frequency calculations were also performed for the studied complexes at the same method; the absence of negative eigenvalues in the corresponding IR spectra assumes that the true minimum on the potential energy surface was successfully achieved.

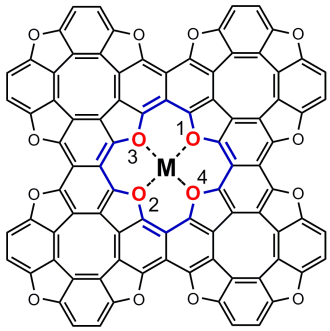

	S
1 M = Cu^{+}	0
2 M = Cu^{2+}	1/2
3 M = Zn^{2+}	0
4 M = Fe^{2+}	0
4 M = Fe^{2+}	1
5 M = Pt^{2+}	0
5 M = Pt^{2+}	1

Fig. 2 Structure of the d-block metal complexes with the tetraoxa[8]circulene based ligand (coordination M–O bonds are shown by the dashed lines, *S* – spin number of the complexes).

The topological analysis of the electron density distribution function $\rho(\mathbf{r})$ at the Bader's level of Quantum Theory of Atoms in Molecules (QTAIM)[19] have also performed for the optimized structures of the studied complexes. The energies of the coordination M–O bonds and of other intermolecular contacts (π-stacking interactions in the sandwich complex **6**) have been calculated by the Espinosa's equation:[20]

$$E = 0.5\, v(\mathbf{r}), \quad (1)$$

where E is the bond energy (a.u), $v(\mathbf{r})$ is the potential energy density (a.u) at the corresponding (3, –1) critical point[19].

The Espinosa's relationship is widely used for the energy estimation of different types of hydrogen,[20b,c] van der Waals,[20d] coordination[20e,f] and homopolar bonds.[20g] The usage of the Bader method makes it possible to describe qualitatively the chemical bond nature based on the signs and values of the electron density Laplacian $\nabla^2\rho(\mathbf{r})$ and of the electron energy density $h_e(\mathbf{r})$ at the corresponding (3, –1) bond critical point in accordance with the following conditions:[19b,21]

1) $\nabla^2\rho(\mathbf{r}) < 0$, $h_e(\mathbf{r}) < 0$ indicates the shared interactions, i.e. weakly polar and nonpolar covalent bonds;

2) $\nabla^2\rho(\mathbf{r}) > 0$, $h_e(\mathbf{r}) < 0$ indicates the intermediate interactions, which include strong hydrogen bonds and most of the coordination bonds;

3) $\nabla^2\rho(\mathbf{r}) > 0$, $h_e(\mathbf{r}) > 0$ indicates the closed shell interactions such as weak hydrogen bonds, Van-der-Waals interactions, ionic bonds.

The binding energy (BE) of a metal cation to the TOC based ligand has been additionally calculated by the following equation in the framework of DFT/B3LYP additive scheme in a gas phase:

$$BE = E(\text{complex}) - [E(M^{n+}) + E(\text{TOC-ligand})].$$

Counterpoise (CP) corrections were applied to all binding

energy values to avoid basis set superposition error (BSSE) [22].

All DFT calculations have been performed using the GAUSSIAN09 software[23]. The QTAIM calculations have been carried out using the AIMAll program package[24].

3. Results and discussion

3.1. Structural features and complexation selectivity

The calculation of the equilibrium geometry parameters showed that the one-decker complexes (Fig. 2) and two-decker sandwich-type complex **6** (Fig. 3) are highly symmetrical compounds and belong to the D_{4h} symmetry point group (excepting less symmetrical complex **4**, which belong to the C_{2h} symmetry point group in the ground triplet state). Thus, the four M–O bonds in the complexes **1–5** (Fig. 2) and eight M–O bonds in sandwich **6** are equivalent by the bond lengths and electronic criteria (Tables 1 and 2). For complex **4** (in which the excited singlet state is higher on 33.5 kcal/mol than the ground triplet state) four coordination bonds are pairwise equivalent (Fig. 2, Table 1). Analogous symmetry reduction is also observed for the platinum complex **5** in the exited triplet state (which is slightly higher on 4.16 kcal/mol than the ground singlet state) (Fig. 2, Table 1). Thus, the central ion coordination sphere represents the square-planar polyhedron for the complexes **1–5** and a proper rectangular prism for the complex **6** in the ground state (whereas for complexes **4**, **5** in the exited state coordination sphere has a planar rhombic form).

The selectivity of the d-block metal complexation with the TOC sheet can be interpreted in terms of the strict correlation between the cation size and macrocycle cavity of the TOC-tetramer (Fig. 1**h**) similarly to the s-block metals complexation with the TOC sheets[16] and to the formation of "crown ethers – metal" complexes[25]. Thus, the TOC-sheet with the 16-crown-4 cavity (diameter of 4.1 Å distance between the two opposite Oxygen atoms) is the most appropriate for the inclusion into this cavity of the small $Cu^{1+,}$ Cu^{2+}, Zn^{2+} and Pt^{2+} ions which have almost equal ionic radii 0.60, 0.57, 0.60 and 0.60 Å, respectively.[26]

Transition metal ions with larger ionic radii can not squeeze into the macrocyclic 16-crown-4 cavity through the strong Coulomb repulsion forces. However, larger ions such as Cd^{2+} ion with an ionic radius of 0.78 Å[26] can simultaneously bind two TOC-sheets forming sandwich-type complex **6** (Fig. 3). It is one of the few examples of the formation of cubic Oxygen coordination sphere with the central transition metal ion. The structure of these transition metal complexes is discussed below in more details.

3.2. QTAIM analysis of M–O interactions in the one-decker square complexes 1–5

Further analysis of the metal-ligand bonding nature was carried out in the framework of Bader's theory formalism[19] for the studied complexes. As can be seen from Table 2, the critical points of M–O bonds are characterized by the positive values of the electron density Laplacian $\nabla^2\rho(\mathbf{r}) > 0$ and by negative values of the Cremer–Kraka electron energy density $h_e(\mathbf{r}) < 0$ that allows us to attribute these M–O bonds to an intermediate type of interactions. In addition, the $|\lambda_1/\lambda_3|$ curvature elements ratio for all M–O bonds varies in the range of 0.154–0.225 (Table 1) i.e. $|\lambda_1/\lambda_3| < 1$ that corresponds to the electron density rarefaction in the interatomic space and corresponds to low-covalence chemical bonds. The covalence degree of the M–O bonds can be measured through the electron density delocalization indices (DI) between the O and M atoms. It should be noted, that for the Pt^{2+}–O bonds in complex **5** in the ground singlet state are observed the highest DI values (0.61, Table 1) indicating a significant number of electron density in the interatomic space. For other M–O bonds, DI values are somewhat smaller and vary in the range 0.33–0.49 (Table 1).

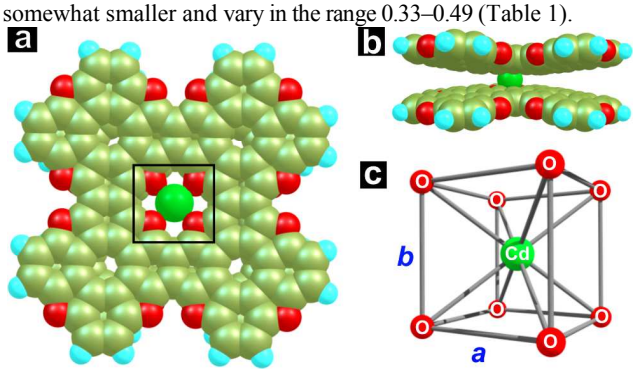

Fig. 3 The optimized structure of the sandwich-type complex **6** $[Cd(TOC)_2]^{2+}$: a – top view, b – side view, c – prism-shaped coordination cage consisting of the Cd^{2+} ion ($a \neq b$).

Obviously, that the degree of the electron density concentration between atoms determines the energy of corresponding interactions. Thus, the total complexation energy of the M–O bonds varies in a narrow range 37–49 kcal/mol (Table 1). The Pt^{2+}–O bonds is characterized by the higher binding energy values defining the great stability of $[Pt(TOC)]^{2+}$ complex **5** in the ground singlet state.

Another criterion for the determining of the M–O bonds stability is an ellipticity parameter (ε)[19c] which is determined from the ratio between the curvature elements ($\lambda_1/\lambda_2 - 1$) According to the Bader's theory the bonds with the high ε values are potentially unstable. As one can see from the Table 1 the ε values for the M–O bonds are rather small (excepting Fe^{2+}–O bonds of the $[Fe(TOC)]^{2+}$ complex **4** in the singlet and triplet states) and vary in a narrow region 0.054–0.114 indicating the M–O bonds dynamic stability. The large ellipticity magnitudes for the Fe^{2+}–O coordination bonds are point out to the dynamic instability of the Fe-containing cycles.

As can be seen from the Table 1 the calculated DI indexes abide by the direct interrelation between the localization indexes (LI) and atomic charge values (q), i. e. increasing of DI leads to the decreasing of the LI and q parameters. The LI criterion evaluates the electron density localization degree in the atomic basin of the central metal ions. For example, the LI index for the unbound (free) Pt^{2+} ion equals to 76e which corresponds to the total number of electrons at all energy levels of the Pt^{2+} ion. After the complexation the LI value decreases to 75.546e; it means that a small portion of the electron density migrates from the atomic basin of the platinum ion into the interatomic space. A similar effect is also observed for coordination M–O bonds in other studied complexes (Table 1). This result can be explained by the effect of the electrostatic polarization which direction (according to the Gauss theorem for ionic systems) is opposite to the direction of the charge transfer. At the same time, the Pt^{2+} (on which a considerable positive charge is concentrated) possesses a

Table 1. The $\rho(\mathbf{r})$ function curvature element values (λ), their relationships ($|\lambda_1/\lambda_3|$ and $\varepsilon = \lambda_1/\lambda_2 - 1$) at the M–O critical point and some electron density localization parameters (DI-delocalization index, LI-localization index, q –atomic Bader's charge)

Complex	S	Bond	λ_1, $e\times a_0^{-5}$ *	λ_2, $e\times a_0^{-5}$	λ_3, $e\times a_0^{-5}$	$\lvert\lambda_1/\lambda_3\rvert$	ε	DI	LI (M)	q
1	0	Cu^{1+} – O	-8.84×10^{-2}	-8.37×10^{-2}	0.4610	0.192	0.055	0.3280	27.496	0.7695
2	1/2	Cu^{2+} – O	-8.83×10^{-2}	-8.38×10^{-2}	0.4614	0.191	0.054	0.3273	27.495	0.7725
3	0	Zn^{2+} – O	-1.01×10^{-1}	-9.46×10^{-2}	0.5565	0.182	0.065	0.3416	27.773	1.4767
4	0	Fe^{2+} – $O_{1,2}$	-1.34×10^{-1}	-4.47×10^{-2}	0.5945	0.225	1.993	0.4564	24.097	1.3338
		Fe^{2+} – $O_{3,4}$	-2.58×10^{-2}	-1.05×10^{-2}	0.4865	0.053	1.455	0.4572		
4	1	Fe^{2+} – O	-0.89×10^{-1}	-0.02×10^{-2}	0.5450	0.163	2.155	0.4380	24.075	1.1625
5	0	Pt^{2+} – O	-1.10×10^{-1}	-9.83×10^{-2}	0.7140	0.154	0.114	0.6099	75.546	1.0820
5	1	Pt^{2+} – $O_{1,2}$	-9.24×10^{-2}	-9.15×10^{-2}	0.6439	0.1435	0.010	0.4900	76.246	0.6449
		Pt^{2+} – $O_{3,4}$	-9.23×10^{-2}	-9.14×10^{-2}	0.6429	0.1436	0.010	0.4896		
6	0	Cd^{2+} – O	-2.94×10^{-2}	-2.78×10^{-2}	0.1660	0.177	0.586	0.2551	45.744	1.5489

S – spin number for the corresponding complex; * a_0 is the Bohr radius.

Table 2. Bond length (d) and selected topological parameters of the electron density distribution function $\rho(\mathbf{r})$ of the M–O bonds

Complex	S	Bond	d, Å	$\rho(\mathbf{r})$, $e\times a_0^{-3}$	$v(\mathbf{r})$, au	$g(\mathbf{r})$, au	$h_e(\mathbf{r})^a$, au	$\nabla^2\rho(\mathbf{r})$, $e\times a_0^{-5}$	E	BE [b]	BE [b]/n	BE [c]
									kcal mol^{-1}			
1	0	Cu^{1+} – O	2.082	6.444×10^{-2}	–0.1196	0.0958	–0.0238	0.2890	–37.51	–384.23	–96.05	–390.27
2	1/2	Cu^{2+} – O	2.081	6.443×10^{-2}	–0.1195	0.0959	–0.0236	0.2893	–37.50	–380.96	–95.24	–386.97
3	0	Zn^{2+} – O	2.042	6.815×10^{-2}	–0.1183	0.1042	–0.0140	0.3604	–37.02	–368.73	–92.18	–374.03
4	0	Fe^{2+} – $O_{1,2}$	2.012	7.249×10^{-2}	–0.1246	0.1143	–0.0107	0.4161	–39.22	–387.54	–96.88	–393.89
		Fe^{2+} – $O_{3,4}$	2.038	5.509×10^{-2}	–0.1074	0.1099	0.0025	0.4514	–33.70			
4	1	Fe^{2+} – O	2.018	6.720×10^{-2}	–0.1210	0.1114	–0.0096	0.4340	–37.96	–398.36	–99.59	–404.95
5	0	Pt^{2+} – O	2.063	9.801×10^{-2}	–0.1560	0.1410	–0.0150	0.5061	–48.95	–465.90	–116.48	–472.75
5	1	Pt^{2+} – $O_{1,2}$	2.138	8.201×10^{-2}	–0.1303	0.1226	–0.0077	0.4600	–40.88	–420.68	–105.18	–426.12
		Pt^{2+} – $O_{3,4}$	2.139	8.190×10^{-2}	–0.1300	0.1224	–0.0076	0.4592	–40.79			
6	0	Cd^{2+} – O	2.554	2.830×10^{-2}	–0.0276	0.0274	–0.0002	0.1085	–8.66	–331.79	–41.47	–338.94

[a] $h_e(\mathbf{r}) = v(\mathbf{r}) + g(\mathbf{r})$, where $g(\mathbf{r})$ is the kinetic energy density at the (3, –1) critical point; $1/4\nabla^2\rho(\mathbf{r}) = 2g(\mathbf{r}) + v(\mathbf{r})$;
[b] BSSE corrected and [c] BSSE uncorrected binding energy of cation to the TOC-ligand at 0 K calculated by the DFT/B3LYP approach in a gas phase without zero-point energy (ZPE) correction; n is the number of the equivalent coordination M–O bonds (n = 4 for complexes **1–5** and n = 8 for sandwich **6**).

significant polarizing ability to disturb the electron shell of the ligand in the direction of the coordination bond.

As a general trend the binding energy (BE) values for the "M–TOC" systems calculated by the direct DFT-method correlate well with the QTAIM predictions. However, such BE values are much higher than the sum of corresponding M–O bonds energies obtained from the QTAIM analysis (Table 2) like it was observed for BE of s-block metals complexes. [16] Such large binding energy differences can be explained by the various approaches to the BE calculation. In the case of DFT-approach the neglect of the solvatation energy takes place (it well known fact that the accounting of the solvatation energy allows to decrease the BE (see for example Ref.[27] But it needs a lot of computational time. Therefore these calculations have not been performed in this work). In contrast, the estimation of complexation energy by the Bader's algorithm is based on the calculation of the potential energy density at the corresponding (3, –1) bond critical point. In this case solvatation energy has a minimal contribution, because of $v(\mathbf{r})$ values slightly depend on solvatation effect.

3.3. QTAIM analysis of M–O interactions in the two-decker sandwich-type complex 6

As we have noted above, the ions which ionic radii are greater than the 16-crown-4 cavity can simultaneously bind of two TOC-tetramers forming the double-decker complexes. We have obtained only a one stable sandwich complex consisting of the Cd^{2+} central ion (Fig. 3) which ionic radii equals to 0.95 Å.[26]

As can be seen from the Fig. 3 the central Cd^{2+} ion is symmetrically chelated between the two TOC-sheets by the "sandwich" principle due to the formation of eight equivalent Cd^{2+}–O bonds with the estimated energies about –8.66 kcal/mol (Table 2).

The Cd^{2+}–O bonds occurring in the sandwich-type complex **6** are characterized by the following conditions: $|\lambda_1/\lambda_3|<1$ and $\nabla^2\rho(\mathbf{r}) > 0$, $h_e(\mathbf{r}) < 0$ (Tables 1 and 2), which corresponds to the intermediate type of interactions similar to the one-decker complexes. Ellipticity of $Cd^{2+}\cdots O$ bonds in the complex **6** equals to 0.586 which is much higher than for the regular complexes **1–3** and **5**, i.e. $Cd^{2+}\cdots O$ bonds are aless dynamically stable than the $Cu^{2+}\cdots O$, $Cu^{+}\cdots O$, $Zn^{2+}\cdots O$ bonds $Pt^{2+}\cdots O$ in the square-planar complexes.

The interplain distance between the two TOC sheets is rather small and equals to b = 3.024 Å (Fig. 3). It means that a considerable accumulation of the local potential energy density in the interplaine space is observed for the complex **6**. The QTAIM analysis has shown that the double-decker complex **6** is

additionally stabilized due to the presence of a number of π-stacking C---C interactions between two TOC parallel plains (Fig. 3). The total energy of these contacts calculated by the Espinosa formula (1) equals to –10.18 kcal mol^{-1}. It should be noted, that upon the presence of these bonds TOC-sheets slightly bent (at about 7°) while in the unbound state TOC-sheets are absolutely planar.

4. Conclusions

The two different types (square planar and sandwich-type) of highly symmetrical transition metal complexes with the tetraoxa[8]circulene-based ligand have been designed in the framework of the density functional theory approach and the quantum theory of atoms in molecules analysis have been performed for their optimized structures.

Our calculations indicate the definite selectivity of the d-block metal ion complexation depending on a strict correlation between the cation radius and size of macrocycle cavity of the tetraoxa[8]circulene-tetramer (like the already known crown ether). It can be useful for the creation of the synthetic ionic channels based on tetraoxa[8]circulene-nanosheets.

The mutual polarization of the transition metal cations and organic ligand leads to the deformation of the electron shell of tetraoxa[8]circulene-based ligand. As a result all coordination M…O bonds occurring in the studied complexes in ground state are characterized by the following conditions: $|\lambda_1/\lambda_3|<1$ and $\nabla^2\rho(\mathbf{r}) > 0$, $h_e(\mathbf{r}) < 0$ that determines an intermediate type of interactions in the framework of Bader's theory formalism.

All the studied complexes are predicted to be very stable because of the high values of ion-to-ligand binding energies. This fact indicates a high binding affinity of tetraoxa[8]circulene-based ligands relative to the d-block metal ions, i.e. tetraoxa[8]circulene-based ligands represent a very sensitive species for the metal ions extraction.

Acknowledgements

All the computations were performed with the resources provided by the Swedish National Infrastructure for Computing (SNIC) at the Parallel Computer Center (PDC) through the project "Multiphysics Modeling of Molecular Materials", SNIC 020/11-23. This research was also supported by the Ministry of Education and Science of Ukraine (project number 0115U000637).

Notes and references

[a] *Bohdan Khmelnytsky National University, Cherkasy, 18031, Ukraine; E-mail: glebchem@rambler.ru, karaush_nataliya@rambler.ru*

[b] *Key Laboratory of Engineering Plastics and Beijing National Laboratory for Molecular Sciences, N2 Beiyijie, Zhongguancun, Beijing 100190, China.*

*†Electronic Supplementary Information (ESI) available: [optimized structure and corresponding Cartesian coordinates for the complexes **1–7**]. See DOI: 10.1039/b000000x/*

‡ The circulenes family includes the synthesized tetraoxa[8]circulenes, azaoxa[8]circulenes, thio[8]circulenes and some theoretically predicted hetero[8]circulenes (see Refs.[8,9]).

1 (*a*) J.-M. Lehn, Supramolecular Chemistry: Concepts and Perspectives, VCH Weinheim, 1995; (*b*) M. Ruben, J. Rojo, F. J. Romero-Salguero, L. H. Uppadine, J.-M. Lehn, *Angew. Chem. Int. Ed.*, 2004, **43**, 3644; (*c*) J.-M. Lehn, *Chem. Soc. Rev.*, 2007, **36**, 151; (*d*) L. Marchiò, N. Marchetti, C. Atzeri, V. Borghesani, M. Remellib, M. Tegoni, *Dalton Trans.*, 2015, **44**, 3237.

2. (a) S.-J. Rymer, S. JB Tendler, C. Bosquillon, C. Washington, C. J. Roberts, Therapeutic Delivery, 2011 **2**, 1043; (b) S. Y. Fung, H. Yang, P. T. Bhola, P. Sadatmousavi, E. Muzar, M. Liu, P. Chen, *Adv. Funct. Mat.*, 2009, **19**, 74; (*c*) X.Q. An, J.C. Yu, RSC Adv. 2011, **1** 1426; (*d*) Y.Q. Sun, Q.O. Wu, G.Q. Shi, *Energy Environ. Sci.*, 2011, **4**, 1113; (*e*) C.X. Guo, G.H. Guai, C.M. Li, *Adv. Energy Mater.*, 2011, **1**, 448; (*f*) M. Dragoman, D. Dragoman, *Prog. Quantum. Electron.*, 2009, **33**, 165; (g) J.N. Tiwari, R.N. Tiwari, K.S. Kim, *Prog. Mater. Sci.*, 2012, **57**, 724; (*h*) L. J. Zhi, Y. Fang, F.Y. Kang, *New Carbon Mater.*, 2011, 26, 5; (*i*) M. Wu, X. Wu, Y. Pei, X.C. Zeng, *Nano Res.*, 2011, 4, 233; (*j*) N. N. Karaush, G. V. Baryshnikov, B. F. Minaev, *Chem. Phys. Lett.*, 2014, **612**, 229.

3. Y. Kang, Z. Zhang, H. Shi, J. Zhang, L. Liang, Q. Wang, H. Agren, Y. Tu, *Nanoscale*, 2014, DOI: 10.1039/c4nr01383b.

4. (*a*) O. Costisor, W. Linert, Metal Mediated Template Synthesis of Ligands, World Scientific Publishing Company, 2004; (*b*) M. C. Thompson, D. H. Busch *J. Am. Chem. Soc.*, 1964, **86**, 213; (c) M. Chastrette, F. Chastrette J.C.S. *Chem. Comm*., 1973, 534; (*d*) M. G. B. Drew, C. V. Knox, S. M. Nelson J. Chem. Soc., *Dalton Trans*., 1980, 942; (e) P. N. Martinho, T. Lemma, B. Gildea, G. Picardi, H. Müller-Bunz, R. J. Forster, T. E. Keyes, G. Redmond, G. G. Morgan, *Angew. Chem. Int. Ed.*, 2012, **51**, 11995.

5. (*a*) E. Breuning, M. Ruben, J.-M. Lehn, F. Renz, Y. Garcia, V. Ksenofontov, P. Gütlich, E. Wegelius, K. Rissanen, *Angew. Chem. Int. Ed.*, 2000, **39**, 2504; (*b*) M. Ruben, E. Breuning, J.-P. Gisselbrecht, J.-M. Lehn, *Angew. Chem. Int. Ed.*, 2000, **39**, 4139; (*c*) S. Stepanow, N. Lin, D. Payer, U. Schlickum, F. Klappenberger, G. Zoppellaro, M. Ruben, H. Brune, J. V. Barth, K. Kern, *Angew. Chem. Int. Ed.*, 2007, **46**, 710; (*d*) M. A. Lingenfelder, H. Spillmann, A. Dmitriev, S. Stepanow, N. Lin, J. V. Barth, K. Kern, *Chem. Eur. J.*, 2004, **10**, 1913; (*c*) M. Ruben, *Angew. Chem. Int. Ed.*, 2005, **44**, 1594; (*e*) R. A. Shiekh, I. A. Rahman, M. A. Malik, N. Luddin, S. M. Masudi1, S. A. Al-Thabaiti, *Int. J. Electrochem. Sci*., 2013, **8**, 6972.

6. (*a*) P. Payra, S.-C. Hung, W.-H. Kwok, D. Johnston, J. Gallucci, M. K. Chan, *Inorg. Chem.*, 2001, **40**, 4036. (*b*) W.-H. Kwok, H. Zhang, P. Payra, M. Duan, S.-C. Hung, D. H. Johnston, J. Gallucci, E. Skrzypczak-Jankun, M. K. Chan, *Inorg. Chem.*, 2000, *39*, 2367. (*c*) P. Payra, H. Zhang, W.-H. Kwok, M. Duan, J. Gallucci, M. K. Chan, *Inorg. Chem.*, 2000, **39**, 1076; (*d*) T. Fekner, J. Gallucci, M. K. Chan, *J. Am. Chem. Soc.*, 2004, **126**, 223.

7. (a) A. Srinivasan, H. Furuta, *Acc. Chem. Res.*, 2005, **38**, 10; (b) N. K. Allampally, C. A. Strassert, L. D. Cola, *Dalton Trans.*, 2012, **41**, 13132; (*c*) M. E. Kosal, J. Chou, S. R. Wilson, K. S. Suslick, *Nature Materials*, 2002, **1**, 118.

8 (*a*) H. Erdtman and H.-E. Högberg, *Chem. Commun.*, 1968, 773; (*b*) H. Erdtman and H.-E. Högberg, *Tetrahedron Lett.*, 1970, 11, 3389; (*c*) H.-E. Högberg, *Acta Chem. Scand.*, 1972, **26**, 309; (*d*) H.-E. Högberg, *Acta Chem. Scand.*, 1973, **27**, 2591; (*e*) J. Eskildsen, T. Reenberg and J. B. Christensen, *Eur. J. Org. Chem.*, 2000, 1637; (*f*) K. Y. Chernichenko, V. V. Sumerin, R. V. Shpanchenko, E. S. Balenkova and V. G. Nenajdenko, *Angew. Chem., Int. Ed.*, 2006, **45**, 7367; (*g*) A. Dadvand, F. Cicoira, K. Y. Chernichenko, E. S. Balenkova, R. M. Osuna, F. Rosei and V. G. Nenajdenko, *Chem. Commun.*, 2008, 5354; (*h*) T. N. Gribanova, N. S. Zefirov and V. I. Minkin, *Pure Appl. Chem.*, 2010, **82**, 1011; (*i*) C. B. Nielsen, T. Brock-Nannestad, T. K. Reenberg, P. Hammershoj, J. B. Christensen, J. W. Stouwdam and M. Pittelkow, *Chem.-Eur. J.*, 2010, **16**, 13030; (*i*) T. B. Tai, V. T. T. Huong and M. T. Nguyen, *Chem. Commun.*, 2013, **49**, 11548; (*j*) M. Plesner, T. Hensel, B. E. Nielsen, F. S. Kamounah, T. Brock-Nannestad, C. B. Nielsen, C. G. Tortzen, O. Hammerich, M. Pittelkow, *Org. Biomol. Chem.*, 2015, **13**, 5937; (*k*) S. Radenković, I. Gutman, P. Bultinck, *J. Phys. Chem. A*, 2012, **116**, 9421; (*l*) E. Kleinpeter, A. Koch, S. Schulz, P. Wacker, *Tetrahedron*, 2014, **70**, 9230.

9 (*a*) B. F. Minaev, G. V. Baryshnikov and V. A. Minaeva, *Comput. Theor. Chem.*, 2011, **972**, 68; (*b*) A. Minaeva, B. F. Minaev, G. V. Baryshnikov, H. Agren and M. Pittelkow, *Vib. Spectrosc.*, 2012, **61**,

156; (*c*) G. V. Baryshnikov, B. F. Minaev, M. Pittelkow, C. B. Nielsen and R. Salcedo, *J. Mol. Model.*, 2013, **19**, 847; (d) N. N. Karaush, B. F. Minaev, G. V. Baryshnikov and V. A. Minaeva, *Opt. Spectroscop.*, 2014, **116**, 33; (*e*) G. V. Baryshnikov, N. N. Karaush, B. F. Minaev, *Chem. Heterocycl. Comp*., 2014, **50**, 349; (*f*) G. V. Baryshnikov, R. R. Valiev, N. N. Karaush, B. F. Minaev, *Phys. Chem. Chem. Phys.*, 2014, **16**, 15367–15374; (*g*) G. V. Baryshnikov, N. N. Karaush, R. R. Valiev, B. F. Minaev, *J. Mol. Model.*, 2015, **21**, 136; (*h*) G. V. Baryshnikov, B.F. Minaev, V. A. Minaeva, *Russ. Chem. Rev.*, 2015, **84**, 455; (*i*) X. Xiong, C.-L. Deng, B. F. Minaev, G. V. Baryshnikov, X.-S. Peng, H. N. C. Wong, *Chem. Asian J.*, 2014, **9**, 1; (*j*) G. Baryshnikov, B. Minaev, M. Pittelkow, C. B. Nielsen, R. Salcedo, *J. Mol. Model*. 2013, **19**, 847; (*k*) G. V. Baryshnikov, V. A. Minaeva, B. F. Minaev, N. N. Karaush, X-D. Xiong, M-D Li, D. L. Phillips, H. N. C. Wong, *Spectrochim. Acta A*, 2015, DOI: 10.1016/j.saa.2015.06.020.

10 (*a*) J. Luo, X. Xu, R. Mao and Q. Miao, *J. Am. Chem. Soc.*, 2012, **134**, 13796−13803; (*b*) K. Nakanishi, D. Fukatsu, K. Takaishi, T. Tsuji, K. Uenaka, K. Kuramochi, T. Kawabata and K. Tsubaki, *J. Am. Chem. Soc.*, 2014, **136**, 7101.

11. (*a*) G. V. Baryshnikov, B. F. Minaev, N. N. Karaush and V. A. Minaeva, *Phys. Chem. Chem. Phys.*, 2014, **16**, 6555; (b) G. Baryshnikov, B. Minaev, N. Karaush, V. Minaeva, *RSC Adv.*, 2014, **4**, 25843; (*c*) N.N. Karaush, G.V. Baryshnikov, B.F. Minaev, *Proc. NAP*, 2014, **3**, 01CBNM01; (*d*) J. Yu, Q. Sun, Y. Kawazoe, P. Jena, *Nanoscale*, 2014, **6**, 14962.

12. (*a*) C. J. Pedersen, *J. Am. Chem. Soc.*, 1967, **89**, 2495; (*b*) C. J. Pedersen, *J. Am. Chem. Soc*., 1967, **89**, 7017; (*c*) C. J. Pedersen, *J. Am. Chem. Soc.*, 1970, **92**, 386; (*d*) C. J. Pedersen, J. *Am. Chem. Soc.*, 1970, **92**, 391; (*e*) C. J. Pedersen, *J. Org. Chem*., 1971, **36**, 254; (*f*) C. J. Pedersen, *J. Org. Chem.*, 1971, **36**, 1690; (*g*) Y. Kobuke, K. Hanji, K. Horiguchi, M. Asada, Y. Nakayama and J. Furukawa, *J. Am. Chem. Soc*., 1976, **98**, 7415.

13 (*a*) Y. Nakamura, N. Aratani, K. Furukawa and A. Osuka, *Tetrahedron*, 2008, **64**, 11433; (*b*) Y. Nakamura, N. Aratani, H. Shinokubo, A. Takagi, T. Kawai, T. Matsumoto, Z. S. Yoon, D. Y. Kim, T. K. Ahn, D. Kim, A. Muranaka, N. Kobayashi and A. Osuka, *J. Am. Chem. Soc.*, 2006, **128**, 4119.

14. (*a*) Z. Shi and N. Lin, *J. Am. Chem. Soc*., 2010, **132**, 10756; (b) S. Banala, RG Huber, T. Müller, M. Fechtel, KR Liedl and B. Kräutler, *Chem. Commun*., 2012, **48**, 4359; (*b*) S. Banala, K. Wurst and B. Kräutler, *J. Porphyrins Phthalocyanines*, 2014, **18**, 116; (*d*) Y. Li, J. Xiao, T. E. Shubina, M. Chen, Z. Shi, M. Schmid, H.-P. Steinruck, J. M. Gottfried and N. Lin, *J. Am. Chem. Soc*., 2012, **134**, 6401; (*e*) V. E. Pushkarev, E. V. Shulishov, Y. V. Tomilov, L. G. Tomilova, *Tetrahedron Lett.*, 2007, **48**, 5269; (*f*) S. Alpugan, Ü. Işci, F. Albrieux, C. Hirel, A. G. Gürek, Y. Bretonniére, V. Ahşena and F. Dumoulin, *Chem. Commun.*, 2014, **50**, 7466.

15. (a) A. S. Filatov, M. A. Petrukhina, *Coord. Chem. Rev.*, 2010, **254**, 2234; (b) M. A. Petrukhina, *Angew. Chem.* 2008, **120**, 1572; (c) M. A. Petrukhina, *Chem. Angew. Int. Ed.* 2008, **47**, 1550; (d) S. N. Spisak, A. V. Zabula, A. S. Filatov, A. Yu. Rogachev, M. A. Petrukhina, *Angew. Chem. Int. Ed.*, 2011, **50**, 8090; (e) S. N. Spisak, N. J. Sumner, A. V. Zabula, A. S. Filatov, A. Yu. Rogachev, M. A. Petrukhina, *Organometallics*, 2013, **32**, 3773; (*f*) A. V. Zabula, S. N. Spisak, A. S. Filatov, V. M. Grigoryants, M. A. Petrukhina, *Chem. Eur. J.*, 2012, **18**, 6476; (g) C. M. Alvarez, R. J. Angelici, A. Sygula, R. Sygula, P. W. Rabideau, *Organometallics*, 2003, **22**, 624; (*h*) P. J. Fagan, J. C. Calabrese, B. Malone, *Science*, 1991, **252**, 1160.

16 N. N. Karaush, G. V. Baryshnikov, B. F. Minaev, *RSC Adv*., 2015, **5**, 24299.

17 (a) A.D.Becke, *J. Chem. Phys.*, 1993, **98**, 5648–5652; (b) C. Lee, W. Yang, R.G. Parr, *Phys. Rev. B*., 1988, **37**, 785–789.

18 P.J. Hay, P.J. Wadt, *J. Phys. Chem*., 1985, **82**, 270–283.

19. (*a*) R. F. W. Bader, Atoms in Molecules. A Quantum Theory, Calendon Press, Oxford, 1990; (*b*) R. F. W. Bader and H. Essen, *J. Chem. Phys.*, 1984, **80**, 1943; (*c*) R. F. W. Bader, T. S. Slee, D. Cremer and E. Kraka, *J. Am. Chem. Soc.*, 1983, **105**, 5061; (*d*) C. L. Firme, O. A. C. Antunes and P. M. Esteves, *Chem. Phys. Lett.*, 2009, **468**, 129.

20 (*a*) E. Espinosa, E. Molins, C. Lecomte, *Chem. Phys. Lett*., 1998, **285**, 170–173; (*b*) E. Espinosa, I. Alkorta, and I. Rozas, *Chem. Phys. Lett.*, 2001, **336**, 457–461; (c) A. O. Borissova, M. Yu. Antipin, H. A. Karapetyan, A. M. Petrosyan, K. A. Lyssenko, *Mendeleev Commun.*, 2010, **20**, 260; (*d*) G. V. Baryshnikov, B. F. Minaev, V. A. Minaeva, V. G. Nenajdenko, *J. Mol. Model.*, 2013, **19**, 4511; (*e*) G. V. Baryshnikov, B. F. Minaev, A. A. Korop, V. A. Minaeva, A. N. Gusev, *Russ. J. Inorg. Chem.*, 2013, **58**, 928–934; (*f*) F. Shahangi, A. N. Chermahini, H. Farrokhpoura, A. Teimouri, *RSC Adv.*, 2015, **5**, 2305; (*g*) L. N. Puntus, K. A. Lyssenko, M. Yu. Antipin, J.-C. G. Bünzli, *Inorg. Chem.*, 2008, **47**, 11095–11107;

21 D. Cremer and E. Kraka, *Croat. Chem. Act*., 1984, **57**, 1259.

22 S. F. Boys, F. Bernardi, *Mol. Phys.*, 1970, **19**, 553.

23 M. J. Frisch, G. W. Trucks, H. B. Schlegel, G. E. Scuseria, M. A. Robb, J. R. Cheeseman, G. Scalmani, V. Barone, B. Mennucci, G. A. Petersson, H. Nakatsuji, M. Caricato, X. Li, H. P. Hratchian, A. F. Izmaylov, J. Bloino, G. Zheng, J. L. Sonnenberg, M. Hada, M. Ehara, K. Toyota, R. Fukuda, J. Hasegawa, M. Ishida, T. Nakajima, Y. Honda, O. Kitao, H. Nakai, T. Vreven, J. A. Montgomery, Jr., J. E. Peralta, F. Ogliaro, M. Bearpark, J. J. Heyd, E. Brothers, K. N. Kudin, V. N. Staroverov, R. Kobayashi, J. Normand, K. Raghavachari, A. Rendell, J. C. Burant, S. S. Iyengar, J. Tomasi, M. Cossi, N. Rega, J. M. Millam, M. Klene, J. E. Knox, J. B. Cross, V. Bakken, C. Adamo, J. Jaramillo, R. Gomperts, R. E. Stratmann, O. Yazyev, A. J. Austin, R. Cammi, C. Pomelli, J. W. Ochterski, R. L. Martin, K. Morokuma, V. G. Zakrzewski, G. A. Voth, P. Salvador, J. J. Dannenberg, S. Dapprich, A. D. Daniels, Ö. Farkas, J. B. Foresman, J. V. Ortiz, J. Cioslowski and D. J. Fox, *Gaussian 09, revision C.02*, Gaussian, Inc., Wallingford, CT 2009.

24 T. A. Keith, www.aim.tkgristmill.com, 2010.

25 (*a*) C. Fiolka, I. Pantenburg, G. Meyer, *Cryst. Growth Des*., 2011, **11**, 5159; (*b*) P. N. Bartlett, M. J. D. Champion, M. E. Light, W. Levason, G. Reid, P. W. Richardson, *Dalton Trans*., 2015, **44**, 2953.

26 R. D. Shannon, *Acta Chrystallogr. A*, 1976, **32**, 751.

27 J. Heo, Bull. Korean Chem. Soc., 2012, 33, 2669.